# Design Developments and Innovations for the I08 SXM Beamline

**Dr Jon Kelly**
The Diamond Light Source
Harwell Science Campus, Didcot, OX11 0DE, UK
jon.kelly@diamond.ac.uk

***Abstract*** **-**The fundamental aim of the I08 beamline project was to build a 20 nm resolution scanning X-ray microscope (SXM). The endstation was procured from the company Bruker; however to reach the optimum performance the whole beamline was optimised for high stability. The novel endstation support was designed to provide a 3 m travel with a straightness of < 50 μm while achieving a vibration amplitude of < 8 nm Peak-Peak integrated from 40-100 Hz. A vibration damping study was performed on the fabricated support frames, in order to minimise the torsional transmission of vibration to neighbouring optics. The best solution found being Viscoelastic constrained layer damping; which was fitted to all the beamline frames. The first beamline optic is cooled via an indium gallium eutectic bath to mechanically decouple the water circuit. This paper gives examples of vibration test data in combination with finite element analysis to refine the designs to meet the demanding specification. The beamline has demonstrated a resolution of 50 nm to date and started to take users.

***Keywords*****:** Vibration, Damping, Viscoelastic, Granite

## 1 Introduction

Synchrotron facilities such as The Diamond Light Source Ltd (DLS) are designed to produce intense beams of light for scientific investigation. Numerous scientific techniques are employed many of which involve focusing the X-rays to spot sizes in the nanometre range. As spot sizes reduce increasingly higher mechanical and thermal stabilities are required. The I08 scanning X-ray microscope (SXM) beamline has been designed for an ultimate spot size and hence resolution of 20 nm. The microscope endstation was procured from Bruker ASC; however to reach the optimum performance the stability of the whole beamline was considered. This paper describes a number of tests performed and factors considered during the design and commissioning of the beamline.

## 2 Mirror Systems

A small beamline frontend aperture of 59 x 59 µrad was chosen to reduce the excess heat load entering the beamline. The modest 100 W at 500 mA heat load incident on the first mirror, allowed the use of indium/gallium eutectic cooling. This was chosen as it mechanically decouples the water circuit from the optic. The mechanical stability of side clamped or internally cooled optics is usually limited by fluid turbulence induced vibration. The mirror systems were procured from Instrument Design Technology Ltd. The in vacuo assembly may be seen in Figure 1. The design of the mirror mount was a collaboration with DLS. A prototype was tested by DLS using a Fizeau interferometer (Ludbrook, 2010) to validate the low strain mirror mounting. The 5 degree of freedom mirror jack system was mounted on a granite block which was firmly clamped directly to the concrete slab providing a comparable stiffness to grouting. The pitch stability of one of the uncooled mirror systems was measured using a differential position vs. time seismometer measurement. The support/drive system has a fundamental resonant frequency of 20 Hz; however this is a X direction translation mode rather than a rotation with an amplitude of ~ 75 nm Peak-Peak with a residual pitch rotation < 50 nrad Peak-Peak (Kelly, 2014). This pitch stability is reasonable for a multi axis system with a small foot print. The low fundamental Eigen frequency is driven by transient vibration sources such as pallet trucks; however the overfilled exit slit makes the microscope spot stability insensitive to this.

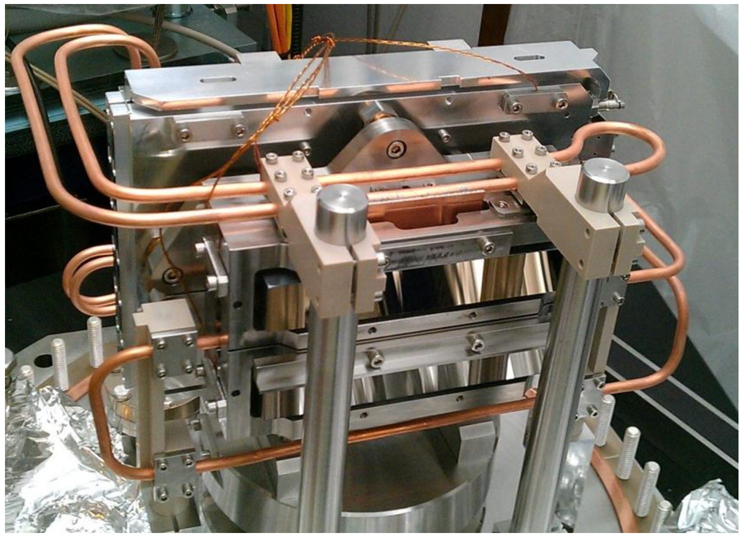

Figure 1: I08 1st mirror assembly, two eutectic cooled mirrors mounted on the common fine pitch plate

# 3 Vibration Damping of Metal Frames

The majority of components on a beamline are supported upon fabricated steel or extruded aluminium frames because they are a cost effective, compact and simple solution. The critical optical components such as mirrors or monochromators tend to be supported upon granite blocks which effectively extend the synchrotron slab up to the optical mechanism. Granite is used due to the inherent damping properties, thermal stability, mechanical stability and high stiffness when in a large solid block.

## 3.1 Bellows Vibration Transmission

Typically the only connection between the critical optical components requiring stability on the sub-microradian level and the neighbouring vessels on metal supports are stainless steel edge welded vacuum bellows, which are assumed to provide adequate isolation. This assumption was tested by the author, by placing horizontal and vertical seismometers (HBA-L1 Institute of Engineering Mechanics, China Earthquake Administration) on a double crystal monochromator (DCM), the neighbouring gas bremsstrahlung collimator (GBC) vessel and the floor. The DCM and then GBC were gently knocked by hand. The amplitude measured on the DCM vessel was only halved when the GBC rather than the DCM was knocked. The edge welded bellows are very ‘soft’ in translation but very stiff in torsion. This is why they are used for motor couplings. The vibration mode of a frame bolted to the floor has both translation and rotation components. So the bellows don’t serve the vibration isolation function well in practice, as the torsional stiffness transmits the rotation motion. This conclusion was the stimulus to find a metal frame vibration damping solution.

## 3.2 Steel Frame Vibration Damping Study

The I08 fabricated frame design has previously been used on at least three other beamlines. The study aim was to investigate simple options which might offer superior performance. A bolted together frame was manufactured to investigate micro-friction damping properties. Side plates were manufactured to investigate the stiffening and friction effects. The plates also allowed the test of various viscoelastic damping materials. Constrained layer damping has been successfully employed to improve the mechanical stability of other synchrotron supports e.g. the ESRF girders (Zhang L., 2001). Finite element analysis (FEA) was performed to highlight the expected modal frequencies and shapes.

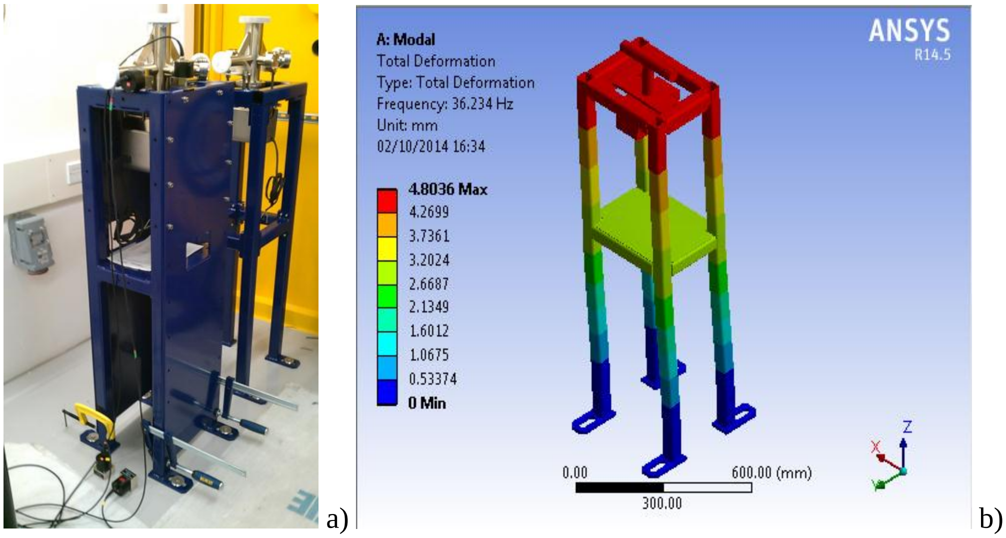


Figure 2: a) Fabricated frame vibration damping study experimental set-up b) ANSYS modal analysis fundamental resonant modes are rocking motions at 35.7 Hz and 36.2 Hz

The two calculated fundamental modes were horizontal translations in X and Z caused by the lower leg flexure at 36.2 Hz and 36.5 Hz (Figure 2b).

Seismometer sensors were positioned on the floor and on the top of the frame as may be seen in Figure 2a. The data contains a lot of structure due to the non-uniform nature of the background vibration but the light blue (horizontal frame sensor) peaks may be clearly seen at 34 Hz and 36 Hz. This is surprisingly close to the FEA data. Lower amplitude resonance peaks may be seen at 17 Hz, 60 Hz, 78 Hz & 86 Hz.

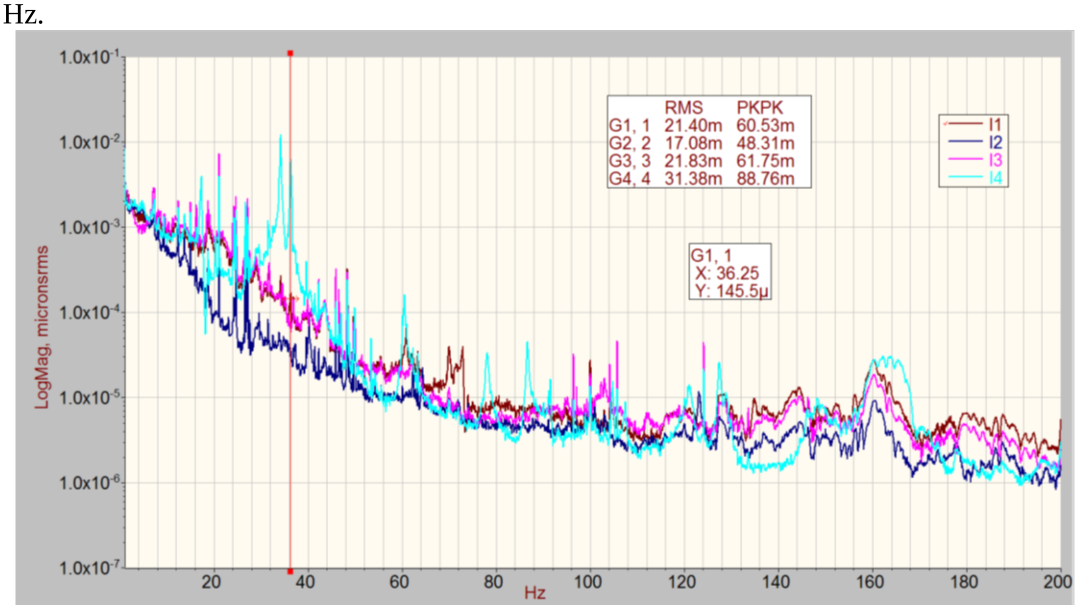


Figure 3: Vibration spectrum, Log µm RMS vs. frequency Hz G1 - Floor Vert, G2 - Floor Horiz - Z Dir, G3 – Frame Vert, G4 – Frame Horiz - Z Dir

Tapping the frame causes the assembly to resonate horizontally. The decay of this waveform indicates the damping properties of the system. As expected the steel fabricated frame & vacuum vessel ‘rings’ for $\geq 5$ s.

The powder coated steel side plates were only bolted at the top of the frame to maximise the relative motion between the plate and the lower legs. This motion caused a shear force at the interface.

With no connection between the plates and the lower legs the vibration spectrum is relatively unchanged; however when clamped hard to the lower legs the increased stiffness pushed the fundamentals up to 56 Hz and 66 Hz.

The metric used to quantify the performance was the time taken for the amplitude of a similar impulse (similar peak measured velocity) to decay to ¼ of the peak amplitude. The results are tabulated below.

Table 1: Fabricated Frame Vibration Study Results

| Test | Test Configuration | ¾ Decay Time |
|---|---|---|
| 1 | Original fabricated frame no extra plates | 3.5 s |
| 2 | Bolted frame of similar dimensions no side plates | 4.0 s |
| 3 | Frame with 2 side plates lightly clamped top & bottom | 0.8 s |
| 4 | Frame with 2 side plates firmly clamped top & bottom | 0.75 s |
| 5 | Frame with 2 side plates firmly clamped top & lightly clamped bottom | 0.45 s |
| 6 | Double sided tape 4 x 25 $mm^2$ under bottom tight clamps | 0.15 s |
| 7 | 2 Layers of double sided tape over 4 x 25 $mm^2$ area | 0.075 s |
| 8 | Roush® RA954-2mil Damping Adhesive 4 x 50mm x 80mm | 0.12 s |

### 3.3 Steel Frame Vibration Damping Study Conclusion

The ratio of the horizontal RMS amplitude integrated over 1 – 200 Hz between the floor and the vessel for the original frame was 1.84 but for the 2 layer double sided sticky tape side plates was 1.15. This simple non-optimised support addition, reduced the vibration decay time by a factor of 47. Double sided tape borrowed from the technician's tool box offers a massive stability improvement for fabricated frames when applied to the vibration anti-node operating in sheer. An optimised frame offers great possibilities for applications requiring light, high performance structures at a very low cost. This viscoelastic double sided tape damping was added to all the I08 beamline frames.

## 4 Granite Endstation Microscope Support

A novel endstation support was designed to provide a 3 m travel with a straightness of < 50 µm. This was required to compensate for the change in focal length with energy of zoneplates. A 4.5 m granite beam was used as the base with a 1.5 m long moving block on to which the microscope was bonded. Four large air pads (FP-R-150300 Nelson Air Corp.) were used as the Z bearing. Vertical adjustment was provided by four wedges with hemispherical washers (202-VRKC Airloc Schrepfer Ltd.). The block was guided by four more air pads, two running on each side of the base granite. The exit slit imaged by the zoneplate was mounted on to a third block, bolted to the base. A photo is given below.

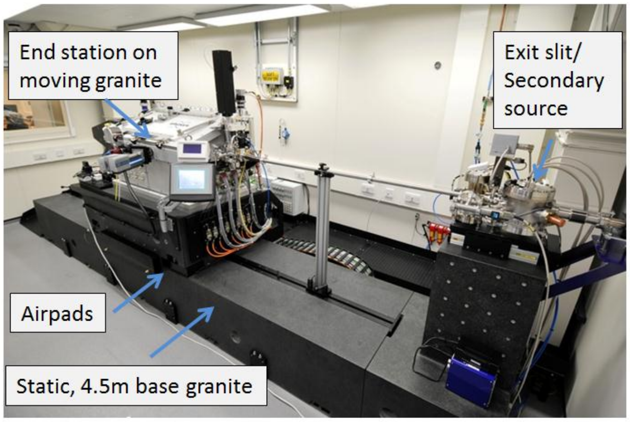


Figure 4: I08 Endstation

### 4.1 Granite to Floor Interface

A study was performed to measure the stability of the numerous static granite support options employed at DLS. The various suppliers use their favoured techniques so measurements were taken to see if one had any particular advantage. . The criterion for a good connection is negligible relative motion between the floor and the granite i.e. good correlation between seismometer data taken on the floor and on the granite. It was conclude that as long as there is a high stiffness connection or a widely distributed connection to the concrete the performance is good. Very similar results were measured for direct grouting to the concrete, bolting of the granite to a grouted plate and even grouting to the flooring rather than direct to the concrete. Good results were achieved for support upon three wedges as long as robust clamps to the concrete were fitted. A low stiffness flooring layer between the concrete and the wedges should be avoided due to the significant reduction in support resonant frequency.

### 4.2 Preliminary Granite Characterisation & Installation

The granite was initially installed in the cabin on the wedges without the microscope nor moving granite. The granite was surveyed into place and all the wedges were brought into contact with the granite, endeavouring to provide an even support. A vibration measurement was taken to check the stability. Example data is given below in Figure 5, for sensors located near the centre of the base granite. The granite was tapped to drive and hence highlight the resonant frequencies.

The base granite data exhibited an amplification factor of about 1 between the floor and the surface, but it did have some surprisingly low resonant frequencies. The vertical peaks (pink) at 62 Hz and 83 Hz and horizontal X direction at 64 Hz. The vertical data shows a first maximum in amplification i.e. the difference between the floor (brown) and the granite (pink) at around 50 Hz. A FEA analysis was carried out to look at the expected resonant modes. If the granite were evenly supported by all the ten wedges the fundamental would be over 100 Hz; However if one assumed that it was only supported by one of the middle wedges and two wedges under the exit slit granite, the first three modes come out as 40 Hz, 63 Hz and 97Hz.

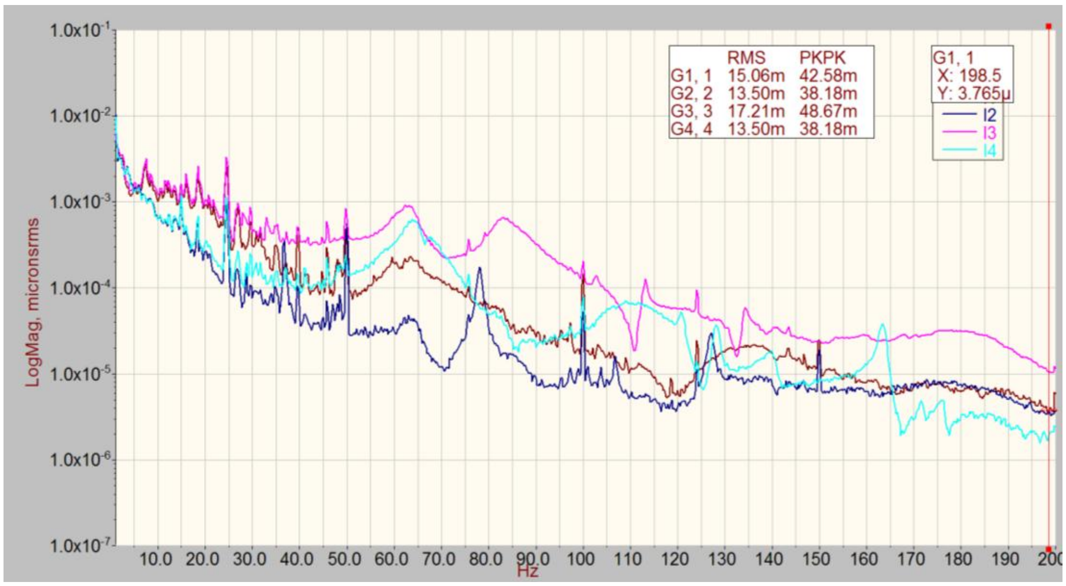


Figure 5: Frequency spectrum taken at the middle of the base granite between wedges, granite tapped to highlight the resonances. G1 - Floor Vert, G2 - Floor Horiz - Z Dir, G3 – Granite Vert, G4 – Granite Horiz - Z Dir

The calculated resonant frequencies depend upon the constraint assumptions; however qualitatively the FEA suggests that the granite is only really supported upon three points. A laser tracker was then used to remeasure the height of the granite surface along its length and interestingly showed a peak in the centre with a height range of 70 µm. This agreed with the FEA support location and when the wedges were double checked agreed with the feel of the screw torque. It appeared that the grease in the wedges and hemispherical washers had flowed over time to cause a change in support and hence physical profile.

There was very good agreement between the vibration measurement, height measurement and the FEA. This information was used to educate the technicians and adjust the installation plan for the final endstation build. The grease was removed from the wedges and the survey was double checked after 30 minutes in case of drift.

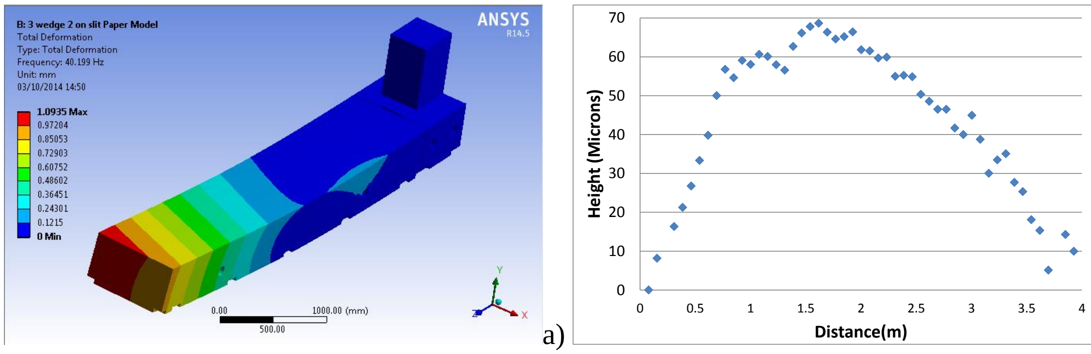


Figure 6: a) FEA data for fundamental 40Hz mode b) Laser tracker height Measurement along base granite upper surface

### 4.3 Microscope Stability Measurement

Vibration data was taken with the microscope fully installed and commissioned. The base granite was bolted down directly to the concrete slab in-between each wedge to supress the resonant modes discussed in the previous section. The moving granite was designed with manual clamps to the base granite for data acquisition stability. The amplification factor between the floor and the moving granite is 1 ± 0.1. The value varies with experimental set-up and vibration background. The horizontal and vertical motion integrated between 1-100 Hz is ~ 50 nm Peak-Peak; which is a typical value for the DLS slab. The majority of the motion is at low frequency. Oscillation below 25 Hz has a wavelength above 148 m (assuming speed of sound in concreate 3700 m/s (Grondzik, 2011)). So the whole endstation if not synchrotron is moving together.

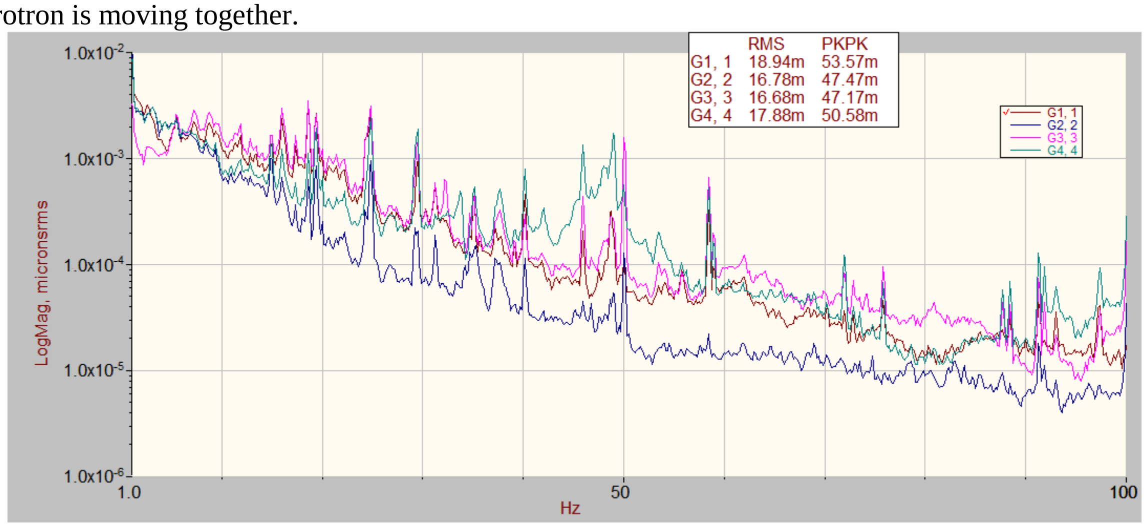


Figure 7: Frequency spectrum taken during the day. G1 - Floor Vert, G2 - Floor Horiz - Z Dir, G3 – Moving Granite Vert, G4 – Moving Granite Horiz - Z Dir

The integrated motion between 25 – 500 Hz is 10 nm in vertical and horizontal. Spectra taken between the moving granite and the exit slit granite show negligible relative motion up to 40 Hz. The integrated motion between 40 – 500 Hz is 6 nm in the vertical and 8 nm in the horizontal. The microscope internal structures are relatively light and stiff and should not amplify motion below their resonant frequencies, although these have not been measured. As the microscope has demonstrated a 50 nm resolution it seems reasonable to quote stability integrated over a reduced frequency range such as 40 – 500 Hz. The ongoing commissioning and use of new zoneplates will enable the optics to focus at 20 nm spot sizes which will be the definitive stability measurement.

## 5 Microscope Support Stiffness and Resonant Frequency

While the microscope position stability is so far sufficient with the typical day time vibration background, it is not possible to operate the microscope when local vibration sources such as a pallet truck appear.

The moving granite has a roll resonance in the X direction at around 60Hz which is clear if the assembly is knocked by hand. The vibration decay time is an order of magnitude lower than a steel frame (See Table 1) at ~ 0.5 s. The support components with the lowest stiffness are the four steel adjustment wedges on top of the air pads. The wedges have a large load capacity but the finite stiffness is defining the resonant frequency. The application of the moving granite clamps, slightly raise the resonant frequency by preloading the system. An FEA study of a similar support using models for the steel wedges with realistic hollow bodies gives a comparable frequency.

The vibration from rolling an empty light pallet truck 5 m away, is conducted by the concrete to drive the 60Hz resonance. A displacement vs. time plot from the seismometers is given below. The total horizontal motion of the floor during the 3 s plot was 0.21 µm and 0.22 µm in the vertical. The total horizontal motion of the moving granite during the 3 s plot was 0.41 µm and 0.33 µm in the vertical. The instantaneous motion was less than this due to the sub 1 Hz drift. The seismometers are not calibrated below 1 Hz.

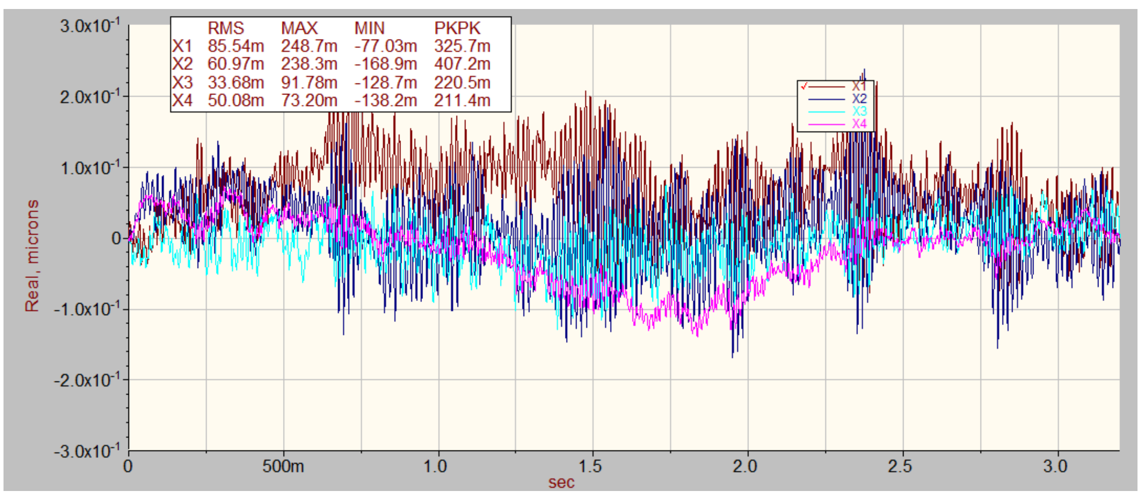


Figure 8: Displacement vs. Time when an empty pallet truck is pushed past outside the cabin. X1 - Moving Granite Vert, X2 - Moving Granite Horiz - Z Dir, X3 Floor –Vert, X4 –Floor - Horiz - Z Dir

The exit slit microscope granite exhibits good coupling up to ~ 40 Hz. The 60 Hz resonance causes a relative motion between the exit slit, microscope zoneplate and sample stage; which is detrimental to the focus stability on the sample.

### 5.1 Vibration Isolation

The microscope moving granite support was designed with spacer plates swapable with elastomer vibration isolation materials. A number of tests with different thickness Sorbothane® and Farrat Isolevel Ltd SG pads were performed. The different spring rates gave different resonant frequencies; however in every test the motion caused by a pallet truck was significantly higher than the original design. The stability when the microscope was floating on the airpads was also tested but gave similar results to the elastomers. The isolation could not be located below the main base granite, because the Z translation of the endstation would cause a significant pitch motion as the centre of mass moved.

The successful isolation of granite blocks from pallet trucks and other sources has been separately verified in tests during the design phase. The significant difference with the final product is the large amount of cabling which ‘shorts’ the vibration isolation. The cables must be constrained within a cable chain guide to enable the 3 m travel but this creates a stiff mechanical link with the floor. The cable chain could be supported by a secondary rail with an increased cable length to fan out to the endstation maintaining the cable flexibility as much as possible, but this was ruled out due to space and aesthetic constraints.

### 5.2 Further Work to Address the Stability Issue

There are a number of avenues to explore to ensure this world class instrument is successfully utilised. The samples may be set-up during the day and the data-sets taken outside normal working hours, or simply repeated if a problem is found with the data set. The user time may be booked around known vibration inducing activities, such as local construction work. The working practices of technicians may be changed to minimise the disturbance. A mechanical upgrade could be performed such as improving the manual clamping of the moving granite or the integration of active vibration damping elements.

## 6 Conclusion

The SXM beamline I08 at the DLS was designed with a holistic approach to stability. The vibration and stability characteristics of all the beamline components, was evaluated and steps taken to mitigate and make improvements during the design and construction phase. A number of these tests and improvements have been described in this paper. The beamline is now routinely demonstrating 50 nm resolution and is taking users.

### Acknowledgements

The design, manufacture, assembly and commissioning of a beamline involves many highly skilled people but special credit must clearly go to Burkhard Kaulich the Principle Beamline Scientist, Kevin Pettet Beamline Technician and Martin Gilbert the Design Engineer.

### References

Grondzik, W. T. (2011). *Mechanical and Electrical Equipment for Buildings, 11th Edition.* John Wiley & Sons.

Kelly, J. (2014). *DLS Report: I08-55-28 (M4 Stability Results).*

Ludbrook, G. D. (2010). A double-pass Fizeau interferometer system for measuring the figure error of large synchrotron optics. *Proceedings of SPIE 7801, Advances in Metrology for X-Ray and EUV Optics III,*.

Zhang L., L. M. (2001). vibration damping systems for magnet girder assembly at the ESRF. *Particle Accelerator Conference*, (pp. 1466-1467). Chicago.